J. Korean Soc. Ind. Appl. Math. Vol.26, No.4, 323–332, 2022 http://doi.org/10.12941/jksiam.2022.26.323

SMOOTHERS BASED ON NONOVERLAPPING DOMAIN DECOMPOSITION METHODS FOR $H(\mathbf{curl})$ PROBLEMS: A NUMERICAL STUDY

DUK-SOON OH[1]

[1]DEPARTMENT OF MATHEMATICS, CHUNGNAM NATIONAL UNIVERSITY, SOUTH KOREA
Email address: duksoon@cnu.ac.kr

ABSTRACT. This paper presents a numerical study on multigrid algorithms of V–cycle type for problems posed in the Hilbert space $H(\mathbf{curl})$ in three dimensions. The multigrid methods are designed for discrete problems originated from the discretization using the hexahedral Nédélec edge element of the lowest-order. Our suggested methods are associated with smoothers constructed by substructuring based on domain decomposition methods of nonoverlapping type. Numerical experiments to demonstrate the robustness and the effectiveness of the suggested algorithms are also provided.

1. INTRODUCTION

Let Ω be a domain that is bounded in $\mathbb{R}^3$. We will work with the $H_0(\mathbf{curl};\Omega)$ Hilbert space which consists of vector fields in the space $(L^2(\Omega))^3$ with curl also in $(L^2(\Omega))^3$ and vanishing tangential components on the boundary $\partial\Omega$ (cf. [1]). We will consider the following variational problem: Find $\boldsymbol{u} \in H_0(\mathbf{curl};\Omega)$ such that

$$a(\boldsymbol{u},\boldsymbol{v}) = (\boldsymbol{f},\boldsymbol{v}), \quad \forall \boldsymbol{v} \in H_0(\mathbf{curl};\Omega), \tag{1.1}$$

where

$$a(\boldsymbol{v},\boldsymbol{w}) = \alpha \cdot (\mathbf{curl}\,\boldsymbol{v}, \mathbf{curl}\,\boldsymbol{w}) + \beta \cdot (\boldsymbol{v},\boldsymbol{w}).$$

Here, $(\cdot,\cdot)$ is the standard inner product on $[L_2(\Omega)]^3$ and we assume that α is nonnegative and β is strictly positive. We also assume that $\boldsymbol{f}$ is a square integrable vector field on Ω, i.e., $\boldsymbol{f} \in (L^2(\Omega))^3$. In this manuscript, we will provide a multigrid framework for solving our model problem (1.1).

The model problem (1.1) is originated from the applications in Maxwell's equation; see [2]. Relevant fast solvers, such as multigrid methods and domain decomposition methods, for problems connected with $H(\mathbf{curl})$ have been discussed in [3–14].

It is well-known that the traditional smoothers for solving the scalar elliptic problems do not work well for vector field problems related to $H(\mathbf{curl})$ and $H(\mathrm{div})$; see [15]. Hence, a

Received by the editors September 4 2022; Revised December 15 2022; Accepted in revised form December 15 2022; Published online December 25 2022.

2020 *Mathematics Subject Classification.* 65N30, 65N55, 65F08.

Key words and phrases. multigrid method, Nédélec finite element, $H(\mathbf{curl})$, nonoverlapping domain decomposition.

special smoothing technique is necessary for vector field problems. Function space splitting methods based on Helmholtz type decompositions pioneered by Hiptmair [7, 16] and Hiptmair and Xu [8] have been considered. In [3,17,18], an overlapping type domain decomposition preconditioner has been applied. We also note that the author and Brenner considered smoothers associated with nonoverlapping type domain decomposition methods for $H(\mathrm{div})$ problems in [19, 20].

In this paper, we propose a V–cycle multigrid method with nonoverlapping domain decomposition smoothers and mainly consider the numerical study that is not covered by theories in [21]. In [21], the author provided the convergence analysis with the assumptions, i.e., convex domain and constant material parameters in (1.1). We test our method with less strict conditions, e.g., jump coefficients for α and β, nonconvex domain. We note that our multigrid method is an $H(\mathbf{curl})$ counterpart of the method in [19, 20] and a nonoverlapping alternative of the method in [3], which requires less computational costs when applying the smoother.

The remainder of this paper is structured as follows. In Section 2, the standard way to discretize our model problem using the hexahedral Nédélec element is introduced. We next present our V–cycle multigrid algorithm in Section 3. Finally, we provide numerical experiments in Section 4.

2. The Discrete Problem

We first consider a triangulation $\mathcal{T}_h$ of Ω into hexahedral elements. The lowest order hexahedral Nédélec element [22, 23] has the following form:

$$\begin{bmatrix} a_1 + a_2 y + a_3 z + a_4 yz \\ b_1 + b_2 z + b_3 x + b_4 zx \\ c_1 + c_2 x + c_3 y + c_4 xy \end{bmatrix}$$

on each hexahedral mesh, where the a_i's, b_i's and c_i's are constants. We note that the twelve degrees of freedom can be completely recovered by the average tangential component on each edge of the element. Using the finite elements, we obtain the following discretized problem for (1.1): Find $\boldsymbol{u}_h \in W_h$ such that

$$a(\boldsymbol{u}_h, \boldsymbol{v}_h) = (\boldsymbol{f}, \boldsymbol{v}_h) \qquad \forall\, \boldsymbol{v}_h \in W_h,$$

where W_h is the Nédélec finite element space of the lowest order.

We define the operator $A : W_h \to W_h'$ in the following way:

$$\langle A\boldsymbol{v}_h, \boldsymbol{w}_h \rangle = a(\boldsymbol{v}_h, \boldsymbol{w}_h) \qquad \forall\, \boldsymbol{v}_h, \boldsymbol{w}_h \in W_h.$$

Here, $\langle \cdot, \cdot, \rangle$ is the canonical bilinear form on $W_h' \times W_h$. We then have the following discrete problem:

$$A\boldsymbol{u}_h = f_h, \tag{2.1}$$

where $f_h \in W_h'$ defined by

$$\langle f_h, \boldsymbol{v}_h \rangle = (\boldsymbol{f}, \boldsymbol{v}_h) \qquad \forall\, \boldsymbol{v}_h \in W_h.$$

3. V-CYCLE MULTIGRID METHOD

In a multigrid setting, we construct a nested sequence of triangulations, $\mathcal{T}_0, \mathcal{T}_1, \cdots$, starting with the initial triangulation $\mathcal{T}_0$ consisting of few hexahedral elements. We assume that $\mathcal{T}_k$ is obtained by uniform subdivision from $\mathcal{T}_{k-1}$. We then define W_k which is the lowest order Nédélec space related to the kth level mesh and the corresponding discrete problem: Find $\boldsymbol{u}_k \in W_k$ such that

$$A_k \boldsymbol{u}_k = f_k. \tag{3.1}$$

Here, f_k is defined by

$$\langle f_k, \boldsymbol{v}_k \rangle = (\boldsymbol{f}, \boldsymbol{v}_k) \qquad \forall\, \boldsymbol{v}_k \in W_k.$$

In order for solving the discrete problem (3.1) using multigrid methods, we need two essential ingredients, intergrid transfer operators and smoothers. We note that everything else can be constructed in a standard way.

Since we are dealing with the nested finite element spaces, the natural injection can be used as the coarse-to-fine operator $I_{k-1}^k : W_{k-1} \longrightarrow W_k$. The fine-to-coarse operator $I_k^{k-1} : W_k' \longrightarrow W_{k-1}'$ is then defined by

$$\langle I_k^{k-1} r, \boldsymbol{v}_{k-1} \rangle = \langle r, I_{k-1}^k \boldsymbol{v}_{k-1} \rangle \qquad \forall\, r \in W_k',\ \boldsymbol{v}_{k-1} \in W_{k-1}.$$

We now focus on the missing piece, smoother. As we are interested in designing nonoverlapping type domain decomposition smoothers, we borrow the standard two level domain decomposition framework, i.e., the coarse level and the fine level that are associated with $\mathcal{T}_{k-1}$ and $\mathcal{T}_k$, respectively.

Before we construct the smoothers, we set up notations for the geometric substructures. Let $\mathcal{E}_{k-1}$, $\mathcal{F}_{k-1}$, and $\mathcal{V}_{k-1}$ be the sets of interior edges, interior faces, and interior vertices of the triangulation $\mathcal{T}_{k-1}$, respectively.

We first consider the interior space. Given any coarse element $T \in \mathcal{T}_{k-1}$, let us define the subspace W_k^T by

$$W_k^T = \{\boldsymbol{v} \in W_k :\ \boldsymbol{v} = \mathbf{0} \text{ on } \Omega \setminus T\}.$$

Let J_T denote the natural injection from W_k^T into W_k. The operator $A_T : W_k^T \to \left(W_k^T\right)'$ is constructed by

$$\langle A_T \boldsymbol{v}, \boldsymbol{w} \rangle = a(\boldsymbol{v}, \boldsymbol{w}) \qquad \forall\, \boldsymbol{v}, \boldsymbol{w} \in W_k^T.$$

For a coarse edge $E \in \mathcal{E}_{k-1}$, there are four coarse elements, $T_E^i, i = 1, 2, 3, 4$, in $\mathcal{T}_{k-1}$ and four coarse faces, $F_E^i, i = 1, 2, 3, 4$, in $\mathcal{F}_{k-1}$, that are sharing E. The edge space W_k^E of W_k is defined as follow:

$$\begin{aligned} W_k^E = \Big\{ \boldsymbol{v} \in W_k : \boldsymbol{v} = \mathbf{0} \ \text{ on } \ \Omega \setminus \Big(\big(\cup_{i=1}^4 T_E^i\big) \bigcup \big(\cup_{j=1}^4 F_E^j\big) \bigcup E \Big), \\ \text{and } a(\boldsymbol{v}, \boldsymbol{w}) = 0 \quad \forall\, \boldsymbol{w} \in \Big(W_k^{T_E^1} + W_k^{T_E^2} + W_k^{T_E^3} + W_k^{T_E^4} \Big) \Big\}. \end{aligned} \tag{3.2}$$

Let $J_E : W_k^E \to W_k$ be the natural injection and the operator $A_E : W_k^E \to \left(W_k^E\right)'$ be defined by

$$\langle A_E \boldsymbol{v}, \boldsymbol{w} \rangle = a(\boldsymbol{v}, \boldsymbol{w}) \qquad \forall\, \boldsymbol{v}, \boldsymbol{w} \in W_k^E.$$

Finally, we define the vertex space W_k^P of W_k. For each coarse vertex $P \in \mathcal{V}_{k-1}$, there are eight elements, $T_P^i, i = 1, \cdots, 8$, in $\mathcal{T}_{k-1}$, twelve faces, $F_P^j, j = 1, \cdots, 12$, in $\mathcal{F}_{k-1}$, and six edges, $E_P^l, l = 1, \cdots, 6$, in $\mathcal{E}_{k-1}$, that have the point P in common. We define the vertex space W_k^P by

$$W_k^P = \Big\{ \boldsymbol{v} \in W_k : \boldsymbol{v} = \mathbf{0} \text{ on } \Omega \setminus \left(\left(\cup_{i=1}^{8} T_P^i \right) \bigcup \left(\cup_{j=1}^{12} F_P^j \right) \bigcup \left(\cup_{l=1}^{6} E_P^l \right) \right), \\ \text{and } a(\boldsymbol{v}, \boldsymbol{w}) = 0 \quad \forall \boldsymbol{w} \in \left(\sum_{i=1}^{8} W_k^{T_P^i} \right) \Big\}.$$

The natural injection $J_P : W_k^P \to W_k$ and the operator A_P are obtained by a similar way to J_E and A_E, respectively.

We now define two smoothers, the edge-based and the vertex-based preconditioners. The edge-based smoother $M_{E,k}^{-1}$ is constructed as follow:

$$M_{E,k}^{-1} = \eta_E \left(\sum_{T \in \mathcal{T}_{k-1}} J_T A_T^{-1} J_T^t + \sum_{E \in \mathcal{E}_{k-1}} J_E A_E^{-1} J_E^t \right).$$

Similarly, the vertex-based smoother $M_{P,k}^{-1}$ is obtained by

$$M_{P,k}^{-1} = \eta_P \left(\sum_{T \in \mathcal{T}_{k-1}} J_T A_T^{-1} J_T^t + \sum_{P \in \mathcal{V}_{k-1}} J_P A_P^{-1} J_P^t \right).$$

Here, η_E and η_P are damping factors and $J_T^t : W_k' \to \left(W_k^T\right)'$, $J_E^t : W_k' \to \left(W_k^E\right)'$, and $J_P^t : W_k' \to \left(W_k^P\right)'$ are the transposes of J_T, J_E, and J_P, respectively. We can decide the damping factors such that

$$\rho\left(M_{E,k}^{-1} A_k\right) \leq 1 \text{ and } \rho\left(M_{P,k}^{-1} A_k\right) \leq 1, \tag{3.3}$$

where $\rho\left(M_{E,k}^{-1} A_k\right)$ and $\rho\left(M_{P,k}^{-1} A_k\right)$ are the spectral radii of $M_{E,k}^{-1} A_k$ and $M_{P,k}^{-1} A_k$, respectively. We note that the conditions in (3.3) are satisfied if $\eta_E \leq 1/12$ and $\eta_P \leq 1/8$.

Putting all together, we can completely determine the multigrid framework. The output $MGV\,(k, g, \boldsymbol{z}_0, m)$ of the kth level (symmetric) multigrid V-cycle algorithm for $A_k \boldsymbol{z} = g$, with initial guess $\boldsymbol{z}_0 \in W_k$ and m smoothing steps, is defined as follows:

For $k = 0$, the result is obtained by using a direct solver:

$$MGV\,(0, g, \boldsymbol{z}_0, m) = A_0^{-1} g.$$

For $k \geq 1$, we set

$$\begin{aligned} \boldsymbol{z}_l &= \boldsymbol{z}_{l-1} + M_k^{-1}\left(g - A_k \boldsymbol{z}_{l-1}\right) \qquad \text{for } l = 1, \cdots, m, \\ \overline{g} &= I_k^{k-1}\left(g - A_k \boldsymbol{z}_m\right), \\ \boldsymbol{z}_{m+1} &= \boldsymbol{z}_m + I_{k-1}^k MGV\left(k-1, \overline{g}, 0, m\right), \\ \boldsymbol{z}_l &= \boldsymbol{z}_{l-1} + M_k^{-1}\left(g - A_k \boldsymbol{z}_{l-1}\right) \qquad \text{for } l = m+2, \cdots, 2m+1. \end{aligned}$$

The output of $MGV\left(k, g, \boldsymbol{z}_0, m\right)$ is $\boldsymbol{z}_{2m+1}$. The smoother M_k is either $M_{E,k}$ or $M_{P,k}$ defined earlier in the current section.

In order to check the efficiency of the algorithm, we consider the following error propagation operator:

$$\mathbb{E}_k^m(\boldsymbol{z} - \boldsymbol{z}_0) = \boldsymbol{z} - MGV(k, g, \boldsymbol{z}_0, m). \tag{3.4}$$

The operator $\mathbb{E}_k^m$ is affiliated with the error after one k^{th} multigrid sweep with m smoothing steps. For more detail, see [24, Chapter 6].

4. Numerical Results

We note that a part of the finite element discretizations has been implemented with the MFEM library [25, 26]. The codes used for the experiments are available at the repository `https://github.com/duksoon-open/MG_ND`.

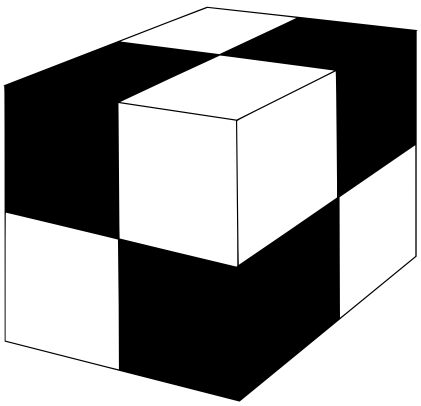

FIGURE 1. Checkerboard distribution of the coefficients

4.1. **Jump Coefficients.** The first experiment is for the cube $\Omega = (-1, 1)^3$. The domain Ω is decomposed into eight identical cubical subdomains and set the subregions as the initial triangulation $\mathcal{T}_0$. We assume that the coefficients α and β are constants in each subdomain in a checkerboard pattern; see Fig. 1. We apply the multigrid algorithms, edge-based method and vertex-based method, introduced in Section 3. We report the contraction numbers by calculating the largest eigenvalue of the operators $\mathbb{E}_k^m$ in (3.4), for $k = 1, \cdots, 4$ and for $m = 1, \cdots, 5$. The results are presented in Table 1 and Table 2. We see that the multigrid methods provide

contraction and are robust to the jump between the interface of the initial mesh. In general, the vertex-based methods perform better than the edge-based methods since we have more computational costs when applying the vertex-based smoothers. For the degrees freedom associated with the coarse faces, we have the same number of sweeps. However, regarding the degrees of freedom related to the coarse edges, the vertex-based methods act twice as many as the edge-based methods.

TABLE 1. Contraction numbers of the V-cycle edge-based methods. α_b and β_b for the black subregions and α_w and β_w for the white subregions as indicated in a checkerboard pattern as in Fig. 1

	$m=1$	$m=2$	$m=3$	$m=4$	$m=5$
	$\alpha_b=0.01, \beta_b=1, \alpha_w=1, \beta_w=1$				
$k=1$	0.905	0.827	0.762	0.709	0.663
$k=2$	0.940	0.908	0.872	0.841	0.811
$k=3$	0.967	0.952	0.935	0.917	0.902
$k=4$	0.981	0.970	0.960	0.955	0.942
	$\alpha_b=0.1, \beta_b=1, \alpha_w=1, \beta_w=1$				
$k=1$	0.905	0.827	0.763	0.710	0.666
$k=2$	0.941	0.910	0.875	0.844	0.807
$k=3$	0.967	0.954	0.937	0.92	0.905
$k=4$	0.980	0.971	0.961	0.956	0.945
	$\alpha_b=1, \beta_b=1, \alpha_w=1, \beta_w=1$				
$k=1$	0.907	0.831	0.769	0.719	0.677
$k=2$	0.944	0.917	0.885	0.858	0.830
$k=3$	0.970	0.959	0.944	0.930	0.917
$k=4$	0.981	0.972	0.965	0.963	0.956
	$\alpha_b=10, \beta_b=1, \alpha_w=1, \beta_w=1$				
$k=1$	0.909	0.836	0.777	0.729	0.690
$k=2$	0.948	0.924	0.896	0.872	0.853
$k=3$	0.972	0.965	0.952	0.941	0.931
$k=4$	0.982	0.974	0.971	0.969	0.966
	$\alpha_b=100, \beta_b=1, \alpha_w=1, \beta_w=1$				
$k=1$	0.910	0.837	0.778	0.731	0.693
$k=2$	0.949	0.926	0.898	0.875	0.857
$k=3$	0.973	0.966	0.954	0.943	0.934
$k=4$	0.982	0.975	0.972	0.970	0.968

TABLE 2. Contraction numbers of the V-cycle vertex-based methods. α_b and β_b for the black subregions and α_w and β_w for the white subregions as indicated in a checkerboard pattern as in Fig. 1

	$m=1$	$m=2$	$m=3$	$m=4$	$m=5$
	$\alpha_b=0.01, \beta_b=1, \alpha_w=1, \beta_w=1$				
$k=1$	0.790	0.624	0.493	0.390	0.308
$k=2$	0.792	0.627	0.495	0.393	0.312
$k=3$	0.791	0.625	0.494	0.391	0.310
$k=4$	0.791	0.626	0.495	0.392	0.317
	$\alpha_b=0.1, \beta_b=1, \alpha_w=1, \beta_w=1$				
$k=1$	0.790	0.624	0.493	0.390	0.308
$k=2$	0.791	0.626	0.494	0.392	0.310
$k=3$	0.791	0.626	0.495	0.392	0.310
$k=4$	0.791	0.626	0.495	0.392	0.311
	$\alpha_b=1, \beta_b=1, \alpha_w=1, \beta_w=1$				
$k=1$	0.790	0.624	0.493	0.390	0.308
$k=2$	0.791	0.626	0.495	0.392	0.310
$k=3$	0.791	0.626	0.495	0.392	0.311
$k=4$	0.791	0.626	0.495	0.392	0.311
	$\alpha_b=10, \beta_b=1, \alpha_w=1, \beta_w=1$				
$k=1$	0.790	0.624	0.493	0.390	0.308
$k=2$	0.791	0.626	0.495	0.392	0.311
$k=3$	0.791	0.626	0.495	0.392	0.311
$k=4$	0.791	0.626	0.495	0.392	0.311
	$\alpha_b=100, \beta_b=1, \alpha_w=1, \beta_w=1$				
$k=1$	0.790	0.624	0.493	0.390	0.308
$k=2$	0.791	0.626	0.495	0.392	0.311
$k=3$	0.791	0.626	0.495	0.393	0.318
$k=4$	0.791	0.632	0.524	0.483	0.429

4.2. **Nonconvex Domains.** In the second set of numerical tests, we consider two kinds of nonconvex domains, $\Omega = (-1,1)^3 \backslash (-1,0)^3$ or $\Omega = (-1,1)^3 \backslash [-1,0] \times [-1,1] \times [-1,0]$; see Figure 2a and Figure 2b. We begin with the initial mesh $\mathcal{T}_0$ which consists of seven or six identical cubes as in Figure 2a and Figure 2b, respectively. We also inductively define the kth level mesh $\mathcal{T}_k$ by a uniform subdivision. Other general settings are similar to those of Section 4.1. We apply our multigrid algorithm for the problem (1.1) on the domains and report the contraction numbers computed in the same manner with the first experiment. As we see the results in the Table 3 and Table 4, the uniform convergences and robustness are observed except for the problem with $k=1$ using the vertex-based smoother.

(A) $\Omega = (-1,1)^3 \backslash [-1,0]^3$ (B) $\Omega = (-1,1)^3 \backslash [-1,0] \times [-1,1] \times [-1,0]$

FIGURE 2. Checkerboard distribution of the coefficients for the nonconvex domains

TABLE 3. Contraction numbers of the V-cycle edge-based methods for the nonconvex domains as in Figure 2. α_b and β_b for the black subregions and α_w and β_w for the white subregions as indicated in a checkerboard pattern.

	Figure 2a					Figure 2b				
	$m=1$	$m=2$	$m=3$	$m=4$	$m=5$	$m=1$	$m=2$	$m=3$	$m=4$	$m=5$
	$\alpha_b = 0.01, \beta_b = 1, \alpha_w = 1, \beta_w = 1$									
$k=1$	0.835	0.702	0.576	0.471	0.420	0.892	0.797	0.710	0.620	0.571
$k=2$	0.940	0.881	0.828	0.785	0.749	0.966	0.937	0.910	0.883	0.855
$k=3$	0.967	0.940	0.918	0.892	0.869	0.981	0.966	0.953	0.935	0.926
$k=4$	0.982	0.969	0.957	0.948	0.934	0.985	0.972	0.961	0.956	0.944
	$\alpha_b = 0.1, \beta_b = 1, \alpha_w = 1, \beta_w = 1$									
$k=1$	0.823	0.682	0.542	0.436	0.390	0.890	0.791	0.705	0.595	0.563
$k=2$	0.943	0.887	0.832	0.796	0.757	0.966	0.940	0.910	0.883	0.860
$k=3$	0.966	0.941	0.918	0.892	0.870	0.980	0.966	0.954	0.938	0.926
$k=4$	0.983	0.970	0.958	0.948	0.936	0.983	0.973	0.962	0.956	0.945
	$\alpha_b = 1, \beta_b = 1, \alpha_w = 1, \beta_w = 1$									
$k=1$	0.799	0.627	0.511	0.419	0.338	0.882	0.766	0.683	0.592	0.501
$k=2$	0.945	0.894	0.844	0.802	0.768	0.968	0.943	0.912	0.881	0.864
$k=3$	0.970	0.942	0.920	0.896	0.876	0.980	0.968	0.956	0.942	0.929
$k=4$	0.984	0.974	0.961	0.950	0.941	0.986	0.975	0.967	0.960	0.955
	$\alpha_b = 10, \beta_b = 1, \alpha_w = 1, \beta_w = 1$									
$k=1$	0.802	0.646	0.523	0.420	0.348	0.870	0.773	0.708	0.627	0.558
$k=2$	0.946	0.896	0.851	0.804	0.773	0.969	0.944	0.914	0.883	0.865
$k=3$	0.972	0.943	0.924	0.902	0.881	0.981	0.970	0.958	0.945	0.933
$k=4$	0.986	0.976	0.964	0.954	0.945	0.987	0.977	0.972	0.966	0.957
	$\alpha_b = 100, \beta_b = 1, \alpha_w = 1, \beta_w = 1$									
$k=1$	0.804	0.651	0.529	0.424	0.354	0.865	0.771	0.716	0.639	0.570
$k=2$	0.947	0.896	0.851	0.805	0.774	0.969	0.944	0.914	0.884	0.865
$k=3$	0.972	0.944	0.924	0.903	0.882	0.981	0.971	0.958	0.946	0.934
$k=4$	0.986	0.976	0.965	0.955	0.946	0.987	0.978	0.971	0.965	0.956

TABLE 4. Contraction numbers of the V-cycle vertex-based methods for the nonconvex domain as in Figure 2. α_b and β_b for the black subregions and α_w and β_w for the white subregions as indicated in a checkerboard pattern.

	Figure 2a					Figure 2b				
	$m=1$	$m=2$	$m=3$	$m=4$	$m=5$	$m=1$	$m=2$	$m=3$	$m=4$	$m=5$
	$\alpha_b=0.01, \beta_b=1, \alpha_w=1, \beta_w=1$									
$k=1$	>1	>1	>1	>1	>1	>1	>1	>1	>1	>1
$k=2$	0.912	0.835	0.765	0.683	0.648	0.880	0.775	0.684	0.606	0.536
$k=3$	0.905	0.825	0.758	0.689	0.622	0.860	0.740	0.634	0.543	0.471
$k=4$	0.912	0.834	0.765	0.697	0.626	0.855	0.725	0.623	0.539	0.459
	$\alpha_b=0.1, \beta_b=1, \alpha_w=1, \beta_w=1$									
$k=1$	>1	>1	>1	>1	>1	>1	>1	>1	>1	>1
$k=2$	0.896	0.808	0.726	0.622	0.598	0.875	0.766	0.671	0.592	0.518
$k=3$	0.878	0.789	0.710	0.629	0.535	0.855	0.731	0.621	0.525	0.452
$k=4$	0.890	0.792	0.703	0.577	0.518	0.850	0.712	0.609	0.526	0.441
	$\alpha_b=1, \beta_b=1, \alpha_w=1, \beta_w=1$									
$k=1$	>1	>1	>1	>1	>1	>1	>1	>1	>1	>1
$k=2$	0.869	0.758	0.660	0.576	0.504	0.858	0.737	0.632	0.544	0.466
$k=3$	0.837	0.705	0.593	0.497	0.425	0.830	0.684	0.568	0.443	0.392
$k=4$	0.827	0.689	0.570	0.479	0.407	0.813	0.639	0.543	0.444	0.354
	$\alpha_b=10, \beta_b=1, \alpha_w=1, \beta_w=1$									
$k=1$	>1	>1	>1	>1	>1	>1	>1	>1	>1	>1
$k=2$	0.863	0.766	0.666	0.591	0.503	0.880	0.774	0.681	0.602	0.525
$k=3$	0.844	0.725	0.613	0.495	0.453	0.845	0.723	0.630	0.529	0.426
$k=4$	0.829	0.706	0.574	0.498	0.420	0.813	0.675	0.619	0.493	0.387
	$\alpha_b=100, \beta_b=1, \alpha_w=1, \beta_w=1$									
$k=1$	>1	>1	>1	>1	>1	>1	>1	>1	>1	>1
$k=2$	0.865	0.772	0.675	0.602	0.515	0.886	0.785	0.697	0.620	0.550
$k=3$	0.849	0.735	0.626	0.509	0.471	0.855	0.738	0.646	0.552	0.427
$k=4$	0.833	0.717	0.590	0.519	0.447	0.810	0.712	0.634	0.529	0.409

ACKNOWLEDGEMENT

This work was supported by the National Research Foundation of Korea (NRF) grant funded by the Korea government (MSIT) (No. 2020R1F1A1A01072168).

REFERENCES

[1] V. Girault and P.-A. Raviart. *Finite element methods for Navier-Stokes equations*, Springer Series in Computational Mathematics 5, Springer-Verlag, Berlin, 1986.

[2] P. B. Monk. *A mixed method for approximating Maxwell's equations*, SIAM J. Numer. Anal., **28** (1991), 1610–1634.

[3] D. N. Arnold, R. S. Falk, and R. Winther. *Multigrid in $H(\mathrm{div})$ and $H(\mathrm{curl})$*. Numer. Math., **85** (2000), 197–217.

[4] J. G. Calvo. *A two-level overlapping Schwarz method for $H(\mathrm{curl})$ in two dimensions with irregular subdomains.* Electron. Trans. Numer. Anal., **44** (2015), 497–521.

[5] J. G. Calvo. *A new coarse space for overlapping Schwarz algorithms for $H(\mathrm{curl})$ problems in three dimensions with irregular subdomains.* Numer. Algorithms, **83** (2020), 885–899.

[6] C. R. Dohrmann and O. B. Widlund. *A BDDC algorithm with deluxe scaling for three-dimensional $H(\mathbf{curl})$ problems.* Comm. Pure Appl. Math., **69** (2016), 745–770.
[7] R. Hiptmair. *Multigrid method for Maxwell's equations.* SIAM J. Numer. Anal., **36** (1999), 204–225.
[8] R. Hiptmair and J. Xu. *Nodal auxiliary space preconditioning in H (curl) and H(div) spaces.* SIAM J. Numer. Anal., **45** (2007), 2483–2509.
[9] Q. Hu and J. Zou. *A nonoverlapping domain decomposition method for Maxwell's equations in three dimensions.* SIAM J. Numer. Anal., **41** (2003), 1682–1708.
[10] T. V. Kolev and P. S. Vassilevski. *Parallel auxiliary space AMG for $H(\mathrm{curl})$ problems.* J. Comput. Math., **27** (2009), 604–623.
[11] Y.-J. Lee, J. Wu, J. Xu, and L. Zikatanov. *Robust subspace correction methods for nearly singular systems.* Math. Models Methods Appl. Sci., **17** (2007), 1937–1963.
[12] A. Toselli. *Overlapping Schwarz methods for Maxwell's equations in three dimensions.* Numer. Math., **86** (2000), 733–752.
[13] A. Toselli. *Domain decomposition methods of dual-primal FETI type for edge element approximations in three dimensions.* C. R. Math. Acad. Sci. Paris, **339** (2004), 673–678.
[14] S. Zampini. *Adaptive BDDC deluxe methods for* $\mathrm{H}(\mathrm{curl})$. Lecture Notes in Computational Science and Engineering, Springer Cham, proceedings of the 23rd DD, Jeju Island, Korea, 2015.
[15] Z. Q. Cai, C. I. Goldstein, and J. E. Pasciak. *Multilevel iteration for mixed finite element systems with penalty.* SIAM J. Sci. Comput., **14** (1993), 1072–1088.
[16] R. Hiptmair. *Multigrid method for $H(\mathrm{div})$ in three dimensions.* Electron. Trans. Numer. Anal., **6** (1997), 133–152.
[17] D. N. Arnold, R. S. Falk, and R. Winther. *Preconditioning in $H(\mathrm{div})$ and applications.* Math. Comp., **66** (1997), 957–984.
[18] D. N. Arnold, R. S. Falk, and R. Winther. *Multigrid preconditioning in $H(\mathrm{div})$ on non-convex polygons.* Comput. Appl. Math., **17** (1998), 303–315.
[19] S. C. Brenner and D.-S. Oh. *Multigrid methods for $H(\mathrm{div})$ in three dimensions with nonoverlapping domain decomposition smoothers* Numer. Linear Algebra Appl., **25** (2018)
[20] S. C. Brenner and D.-S. Oh. *A smoother based on nonoverlapping domain decomposition methods for $H(\mathrm{div})$ problems: a numerical study.* Lecture Notes in Computational Science and Engineering, Springer Cham, proceedings of the 24th DD, Svalbard, Norway, 2017.
[21] D.-S. Oh. *Multigrid methods for 3D H(curl) problems with nonoverlapping domain decomposition smoothers.*, 2022. submitted, arXiv:2205.05840.
[22] P. Monk. *Finite element methods for Maxwell's equations*. Numerical Mathematics and Scientific Computation. Oxford University Press, New York, 2003.
[23] J.-C. Nédélec. *Mixed finite elements in* $\mathbf{R}^3$. Numer. Math., **35** (1980), 315–341.
[24] S. C. Brenner and L. R. Scott. *The mathematical theory of finite element methods* Texts in Applied Mathematics, Springer, New York, 2008.
[25] R. Anderson, J. Andrej, A. Barker, J. Bramwell, J.-S. Camier, J. C. V. Dobrev, Y. Dudouit, A. Fisher, T. Kolev, W. Pazner, M. Stowell, V. Tomov, I. Akkerman, J. Dahm, D. Medina, and S. Zampini. *MFEM: A modular finite element library.* Computers & Mathematics with Applications, **81** (2021), 42–74.
[26] *MFEM: Modular finite element methods [Software].* `mfem.org`.